Downloaded from orbit.dtu.dk on: Apr 28, 2024

DTU Library

Fluorescent probes and degraders of the sterol transport protein Aster-A

He, Nianzhe; Depta, Laura; Sievers, Sonja; Laraia, Luca

Published in:
Bioorganic and Medicinal Chemistry

Link to article, DOI:
10.1016/j.bmc.2024.117673

Publication date:
2024

Document Version
Publisher's PDF, also known as Version of record

Link back to DTU Orbit

Citation (APA):
He, N., Depta, L., Sievers, S., & Laraia, L. (2024). Fluorescent probes and degraders of the sterol transport protein Aster-A. *Bioorganic and Medicinal Chemistry*, *103*, Article 117673. https://doi.org/10.1016/j.bmc.2024.117673

General rights
Copyright and moral rights for the publications made accessible in the public portal are retained by the authors and/or other copyright owners and it is a condition of accessing publications that users recognise and abide by the legal requirements associated with these rights.

- Users may download and print one copy of any publication from the public portal for the purpose of private study or research.
- You may not further distribute the material or use it for any profit-making activity or commercial gain
- You may freely distribute the URL identifying the publication in the public portal

If you believe that this document breaches copyright please contact us providing details, and we will remove access to the work immediately and investigate your claim.

Bioorg. Med. Chem. 103 (2024) 117673

Contents lists available at ScienceDirect

Bioorganic & Medicinal Chemistry

journal homepage: www.elsevier.com/locate/bmc

Fluorescent probes and degraders of the sterol transport protein Aster-A

Nianzhe He [a,1], Laura Depta [a,1], Sonja Sievers [b], Luca Laraia [a,*]

[a] Department of Chemistry, Technical University of Denmark, Kemitorvet 207, 2800 Kgs. Lyngby, Denmark
[b] Max Planck Institute of molecular physiology, Otto-Hahn-Strasse 11, Dortmund, Germany

ARTICLE INFO

Keywords:
Fluorescent probes
Cholesterol transport
Targeted protein degradation

ABSTRACT

Our understanding of sterol transport proteins (STPs) has increased exponentially in the last decades with advances in the cellular and structural biology of these important proteins. However, small molecule probes have only recently been developed for a few selected STPs. Here we describe the synthesis and evaluation of potential proteolysis-targeting chimeras (PROTACs) based on inhibitors of the STP Aster-A. Based on the reported Aster-A inhibitor autogramin-2, ten PROTACs were synthesized. Pomalidomide-based PROTACs functioned as fluorescent probes due to the intrinsic fluorescent properties of the aminophthalimide core, which in some cases was significantly enhanced upon Aster-A binding. Most PROTACs maintained excellent binary affinity to Aster-A, and one compound, **NGF3**, showed promising Aster-A degradation in cells. The tools developed here lay the foundation for optimizing Aster-A fluorescent probes and degraders and studying its activity and function in vitro and in cells.

1. Introduction

Intracellular sterol transport proteins (STPs) are responsible for the non-vesicular transport of sterols between specific organelles.[1–3] This transport is mediated by three proteins families: the ORPs, the STARDs and the Asters. The Asters have been shown to transport cholesterol from the plasma membrane (PM) to the endoplasmic reticulum (ER),[4] however several reports suggest that they have additional functions that are specific to each family member. Aster-A and -C have both been suggested to play a role in autophagosome biogenesis, while Aster-B has been shown to regulate mitochondrial sterol transport,[5] and Aster-C has been suggested to regulate mTOR activity.[6] To complicate matters further, the specific substrates of each Aster may not be limited to sterols, with Aster-B reported to transfer carotenoids.[7] One of the major challenges in studying STPs is the functional redundancy observed within this protein class.[8,9] Therefore knock-down or knock-out cell lines may not be suitable tools to address all of their functions, given the time allowed for cells to adapt.

Small molecule inhibitors offer a way to specifically probe the sterol transport function of an STP, while acting in a rapid and reversible manner.[1] However, selectivity amongst the structurally-related STPs has been challenging to achieve, and infrequently measured. This has changed in the last years, as several groups have reported inhibitors of all three Asters,[10] with potent and selective inhibitors of Aster-A and Aster-C now available.[9,11] More recently, a selectivity panel aimed at measuring activity of a given compound against most sterol-binding ORPs, STARDs and Asters has also been developed, enabling more efficient profiling and characterization of STP ligands.[12] In addition to inhibitors, compounds able to induce the cellular degradation of a target protein are also gaining significant interest. These include proteolysis-, lysosome- or autophagosome-targeting chimeras (PROTACs, LYTACs and AUTACs, respectively).[13–15] However, while certain natural product inhibitors of the STP OSBP lead to its proteasomal degradation,[16] no degrader of an Aster or STARD has been reported to date.

We report the synthesis and profiling of Aster-A targeted PROTACs, designed to engage both Cereblon (CRBN) and von Hippel Lindau (VHL) E3 ligases. While most ligands maintained good to excellent target binding in vitro and several acted as autophagy inhibitors in cells, only one ligand degraded Aster-A in HeLa cells. Notably, CRBN-recruiting PROTACs displayed fluorescence through the pomalidomide aminophthalimide core, which in some cases increased significantly upon Aster-A binding. This enabled the measurement of K_ds in biophysical measurements, and to image cell uptake using fluorescence imaging. As such, the Aster-A probes developed can serve multiple purposes

* Corresponding author.
E-mail address: luclar@kemi.dtu.dk (L. Laraia).
[1] authors contributed equally to this work

https://doi.org/10.1016/j.bmc.2024.117673
Received 12 January 2024; Received in revised form 26 February 2024; Accepted 1 March 2024
Available online 2 March 2024
0968-0896/© 2024 The Authors. Published by Elsevier Ltd. This is an open access article under the CC BY license (http://creativecommons.org/licenses/by/4.0/).

depending on the need. We advocate for a more comprehensive exploitation of the pomalidomide fluorescent properties, given their ubiquitous presence in PROTAC research.

2. Results and discussion

We initially designed our putative Aster-A PROTACs based on reported Aster-A inhibitors, the autogramins (Figure 1a).[9] Previous reports highlighted a position of the core scaffold where substitution was tolerated, and addition of a polyethyleneglycol (PEG) linker did not adversely affect activity. Therefore, we designed compounds based on this scaffold, employing different alkyl- and PEG-based linkers, and coupled these to two E3 ligase recruiting ligands (Figure 1b).[17–19] The choice of flexible linkers was deliberate, to better sample the conformational space around these potential degraders. Pomalidomide and VH032 were chosen to recruit CRBN and VHL E3 ligases, respectively. In total, we generated a proof-of-concept library of 10 potential PROTACs based on these design principles (see SI Figures 1 and 2 for syntheses).

We initially evaluated our compounds for their ability to inhibit the interaction of 22-NBD-cholesterol (22-NBD-Chol) with Aster-A.[9,11] Two out of three VHL-based PROTACs (**NGV1** and **−2**) showed activity in the low μM range, in line with autogramin-2 (Figure 2a and Table 1). Interestingly, **NGV3**, with an alkyl linker consisting of 9 carbon atoms, did not show any activity. We initially speculated that this may be a result of unfavourable solvent interactions of an exposed hydrophobic linker. Notably, **NGV1**, which has a shorter alkyl linker, retained inhibitory properties. The CRBN-recruiting PROTAC candidates could not be tested in this set-up, as they absorb light and can be excited in the 400–450 nm range (SI Figure 3) to emit fluorescence through the pomalidomide aminophthalimide core, which interfered with the 22-NBD-Chol fluorescence. However, we speculated that this property would enable us to detect direct binding to Aster-A by monitoring changes in fluorescence intensity (FI) or fluorescence polarization (FP) upon ligand binding. Interestingly, although the aminophthalimide fluorescence has been used to determine cellular uptake of pomalidomide-based PROTACs,[20,21] to the best of our knowledge no reports of using this scaffold to develop biophysical binding assays is known.

We initially titrated all pomalidomide-based compounds (**NGF1-7**) against increasing concentrations of Aster-A, using linker-pomalidomide conjugates lacking Aster-A ligands as negative controls. Several compounds showed increased FI with increasing Aster-A concentrations, enabling the determination of dissociation constants (K_d, Figure 2b). Importantly, the change in fluorescence was not a result in the change in fluorescence emission maxima, but rather an increase in total fluorescence upon binding (Figure 2c and SI Figure 4). These compounds can thus be considered the first "turn-on" fluorescent probes for Aster-A. Compounds **NGF3, −4, −6** and **−7** displayed K_ds in the sub-100 nM range, highlighting tight binding to Aster-A (Table 1). **NGF5**, which contains a long alkyl linker similarly to **NGV3**, was also inactive, confirming the SAR that suggests longer alkyl linkers to be unfavourable.

Interestingly, the FI binding data showed that **NGF2** did not show an increase in fluorescence with increasing Aster-A concentrations, suggesting a lack of binding. However, an alternative explanation was that no new interactions with Aster-A were formed, leading to a lack of turn-on fluorescence properties. To address this, we measured FP, which is independent of total fluorescence (Figure 2d). Ligands that were active in the FI measurements displayed similar K_d values in the FP measurements (Table 1). Notably, **NGF2** showed tight binding to Aster-A with a $K_d = 149$ nM, which is in stark contrast to the FI data, and supports the notion that, while it a suitable FP probe, it does not display turn-on fluorescence properties. To confirm these results in an orthogonal assay, thermal shift measurements were carried out (Figure 2e and Table 1).[9,11] These confirmed the FP results, where compounds that displayed tight binding by FP also caused a larger change in thermal stability (4 – 7 °C), whereas inactive compounds showed low thermal shifts (<1.6 °C).

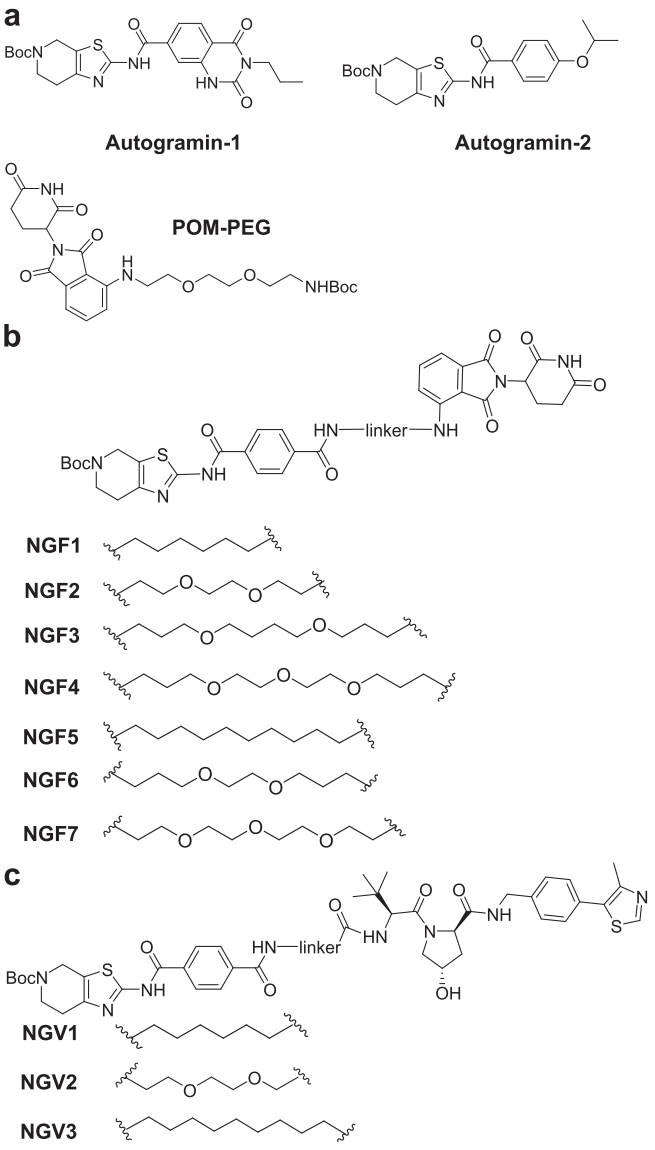

Figure 1. Design strategy for Aster-A PROTACs; (a) structures of reported Aster-A inhibitors; (b) structures of designed PROTACs **NGF1-7** and **NGV1-3**. Please see SI Figures 1 and 2 for syntheses.

To determine the selectivity of the newly developed Aster-A probes, we titrated **NGF3** against a panel of sterol transport proteins (Figure 2f).[12] This revealed that **NGF3** displayed no binding towards the sterol binding domains of Aster-B and -C, as well as STARD1 and good selectivity (≥10-fold) over ORP1 and ORP2. **NGF1-7** were subsequently titrated against ORP1 to determine whether the linker may play a role in further enhancing selectivity towards Aster-A over ORP1. All ligands showed similar binding affinities towards ORP1, as assessed by FI and FP, with the exception of **NGF7**, which displayed equivalent tight binding to both Aster-A and ORP1, and is thus less suitable as a selective probe (SI Figure 5a and 5b). To highlight the utility of the fluorescent probes, we sought to develop competitive FI, against which new Aster-A inhibitors could be screened in the future. To this end, we titrated different concentrations of **NGF3** against Aster-A, which revealed that 100 nM was the optimal concentration to maintain a large assay window (SI Figure 5c). Control compounds autogramin-2 and non-selective sterol transport protein inhibitor U18666A were tested as competitors, revealing IC_{50}s which are similar to the FP assay employing 22-NBD-Chol as a tracer (SI Figure 5d and Table 1). Similar results were obtained using **NGV1-3** as competitors (SI Figure 5e and Table 1), further

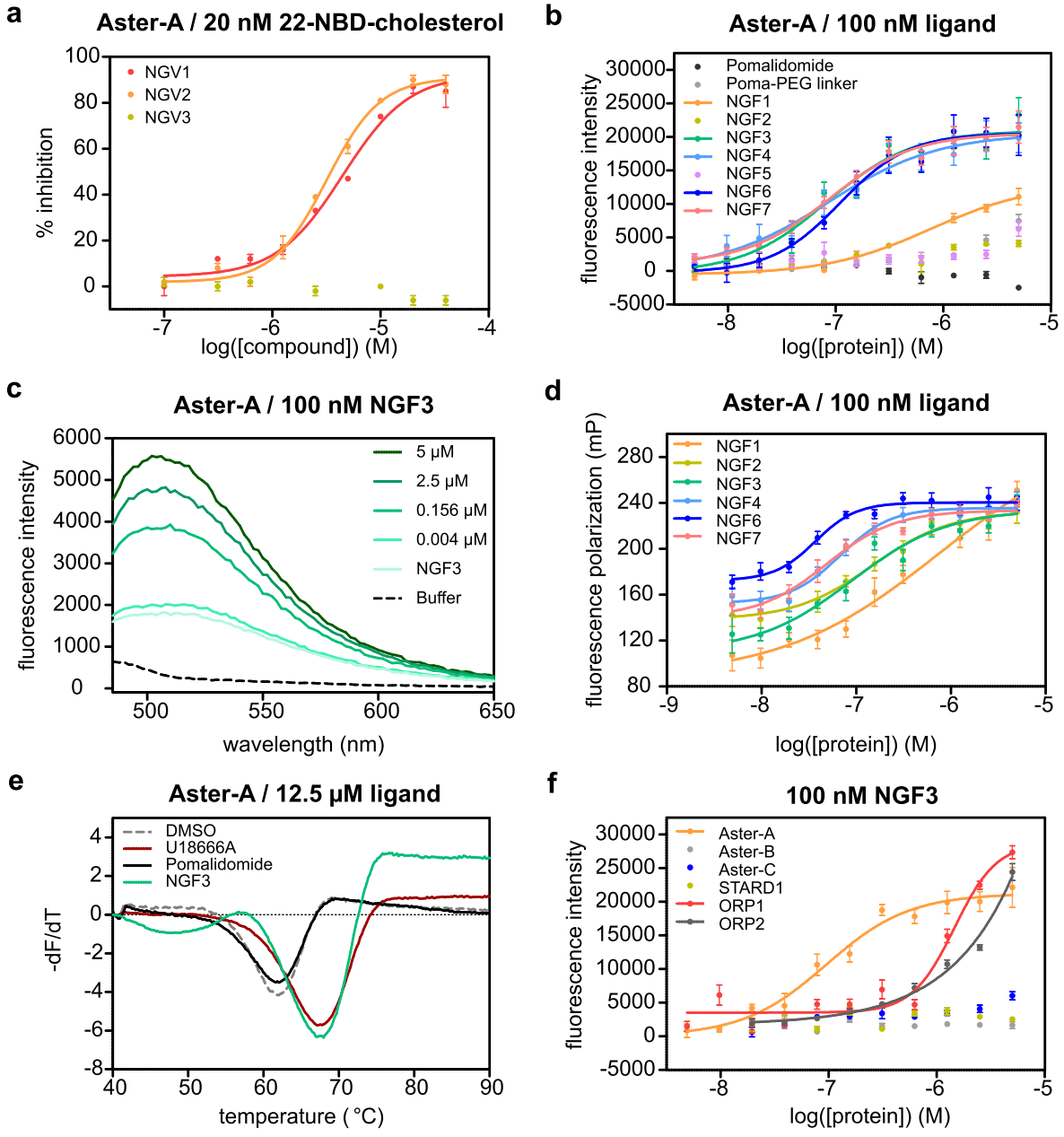

Figure 2. Biophysical evaluation of Aster-A bi-functional molecules. (a) Inhibition of the interaction of 22-NBD-Chol (20 nM) and Aster-A (500 nM) by **NGV1-3** as assessed by FP; (b) titration of all pomalidomide-based ligands against Aster-A assessed by FI; (c) Fluorescence emission spectra of **NGF3** (100 nM) in the presence of increasing concentrations of Aster-A; (d) the same titration as in (b), assessed by FP; (e) thermal stability of Aster-A in presence or absence of ligands, assessed by differential scanning fluorimetry; (f) Titration of NGF3 (100 nM) against a panel of sterol transport proteins assessed by FI. All data is $N = 2$ and n = 3, representative experiments shown.

Table 1
Summary of biophysical data of bi-functional molecules and control compounds tested against Aster-A. FP = fluorescence polarization, DSF = differential scanning fluorimetry. All data is the mean of three independent experiments.[a]NGF2 did not display any enhanced fluorescence upon binding. [b]Data obtained from reference 11.

	FI - K_D [nM]	FP - K_D [nM]	DSF - ΔT_m [° C]	FI - IC_{50} [nM]	FP - IC_{50} [nM]
				competitive - NGF3	competitive – 22-NBD-chol
Pomalidomide	> 5000	> 5000	0.1		
POM-PEG	> 5000	> 5000	0.3		
NGF1	765	745	3.2		
NGF2	> 5000[a]	149	4.0		
NGF3	83	90	5.7		
NGF4	86	68	5.8		
NGF5	> 5000	> 5000	1.2		
NGF6	110	37	5.0		
NGF7	88	49	4.9		
Autogramin-2			6.8	1181	1930[b]
U18666A			5.6	1155	1842
Astercin-1			0.2	> 10000	>10000[b]
NGV1			3.6	2753	4677
NGV2			4.4	1470	3697
NGV3			1.6	> 10000	>10000

highlighting the suitability of **NGF3** as a fluorescent probe in biophysical assays.

To understand the linker requirements for probe binding to Aster-A and the resulting differences in fluorescent behaviour, we performed docking against a humanized homology model of a reported x-ray crystal structure of mouse Aster-A (PDB: 6GQF).[4] This showed that in all cases the autogramin core bound deeply in the sterol binding domain, as previously reported,[9] while the linkers were mostly solvent exposed (Figure 3). However, **NGF2**, which contains the shortest ethylene glycol linker and did not display turn-on fluorescence, was predicted to not engage in productive interactions through its aminophthalimide fluorophore (Figure 3a). This is in contrast to **NGF3** and **−4** which display both predicted polar interactions through the linker, and a key hydrogen bond network with Arg369 (Figure 3b and 3c, respectively), providing a plausible explanation for their turn-on fluorescent properties.

Following this, we sought to determine whether the fluorescent properties of our probes could be used to qualitatively determine their cell permeability, as previously described for other aminophthalimide-based PROTACs.[20,21] Fluorescence and brightfield imaging of HeLa cells treated with the **NGF** compounds showed that intracellular fluorescence could clearly be observed for certain derivatives (Figure 4 and SI Figure 6). Interestingly, **NGF1** showed the highest degree of intracellular fluorescence, despite having a lower binding affinity (K_d = 750 nM) in biophysical measurements and being a worse turn-on fluorescent probe, when compared to **NGF2** and **NGF3**. This suggests that the fluorescence is due to increased cellular uptake, most likely a result of the alkyl linker, which is known to increase permeability compared to more hydrophilic PEG linkers. However, we cannot conclusively determine the effect of compound binding to Aster-A in cells on the intracellular fluorescence, and as such fluorescence intensity may not directly correlate with uptake, in this case. The investigation of the intracellular properties of aminophthalimide Autogramin-2 will be the subject of further study and will be reported in due course. The fact that PROTACs show cell permeability is promising, as many reports in the field highlight poor cell permeability of PROTACs due to their large molecular weight and the presence of numerous hydrogen bond donors and acceptors.

Having confirmed that the designed Aster-A PROTACs maintain good binding affinities towards Aster-A, and displayed encouraging evidence of cell permeability we tested the Aster-A degradation ability of all PROTAC candidates in HeLa cells by Western blot, probing with an Aster-A antibody. Of all candidates tested, only **NGF3** degraded Aster-A, with an approximate reduction in Aster-A levels of 50 % at 10 μM. The degradation was also dose-dependent, with a DC_{50} = 4.8 μM and a D_{max} = 60 %. Following this, the mechanism of the degradation of Aster-A by

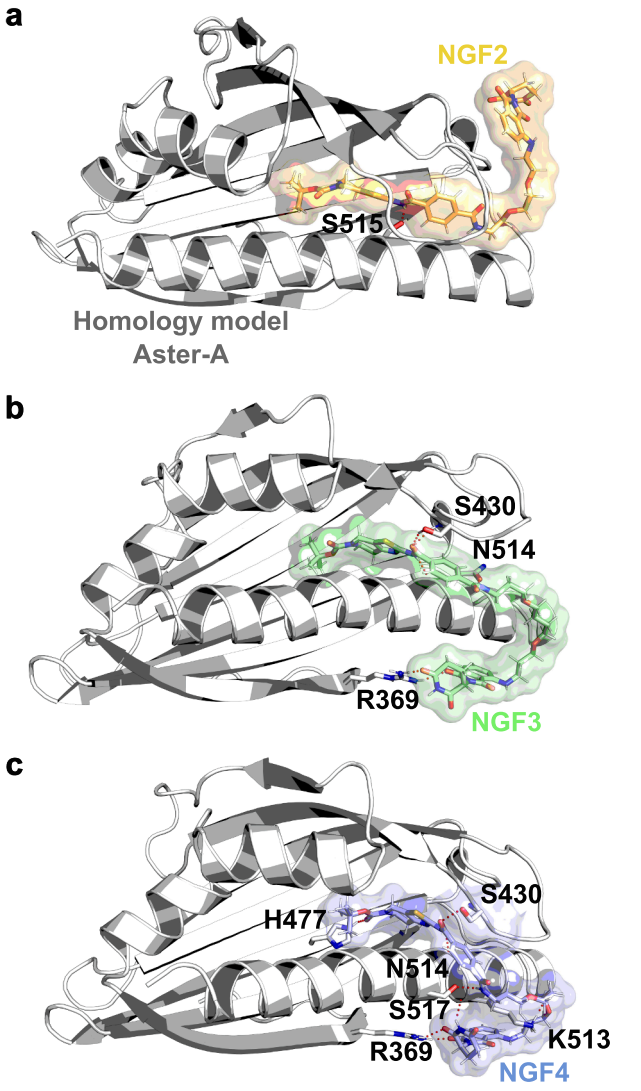

Figure 3. Predicted binding modes of NGF-2, −3 and −4, determined by docking to a humanized homology model of a mouse Aster-A x-ray crystal structure (PDB: 6GQF). Most represented binding modes for **NGF2** (a), **NGF3** (b) and **NGF4** (c) shown.

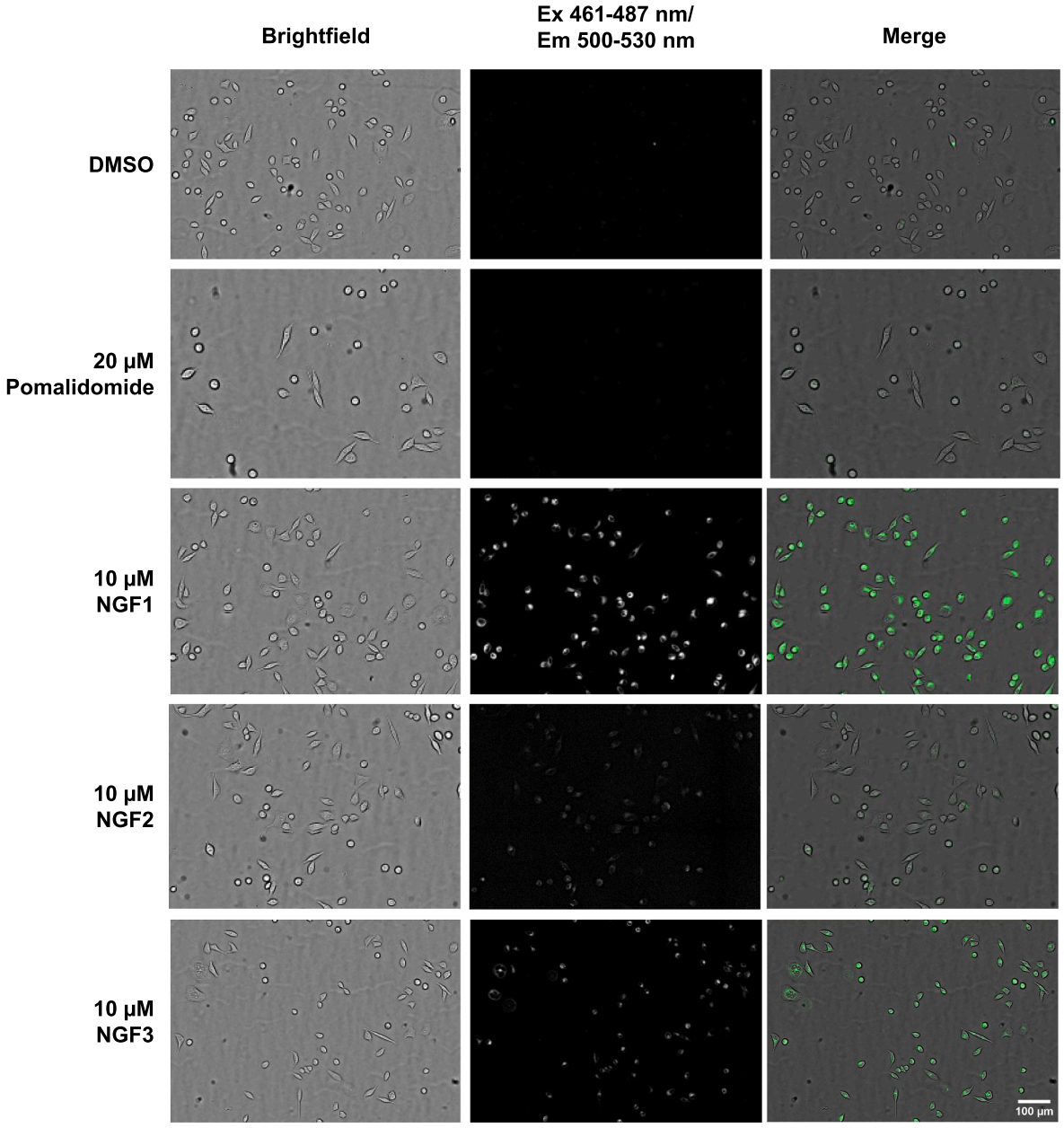

Figure 4. Fluorescent and brightfield imaging of HeLa cells treated with aminophthalimide-based Aster-A probes. Cells were treated with the annotated concentration of compounds for 1 h, before imaging using a Tecan Spark Cyto; N = 3, representative images shown.

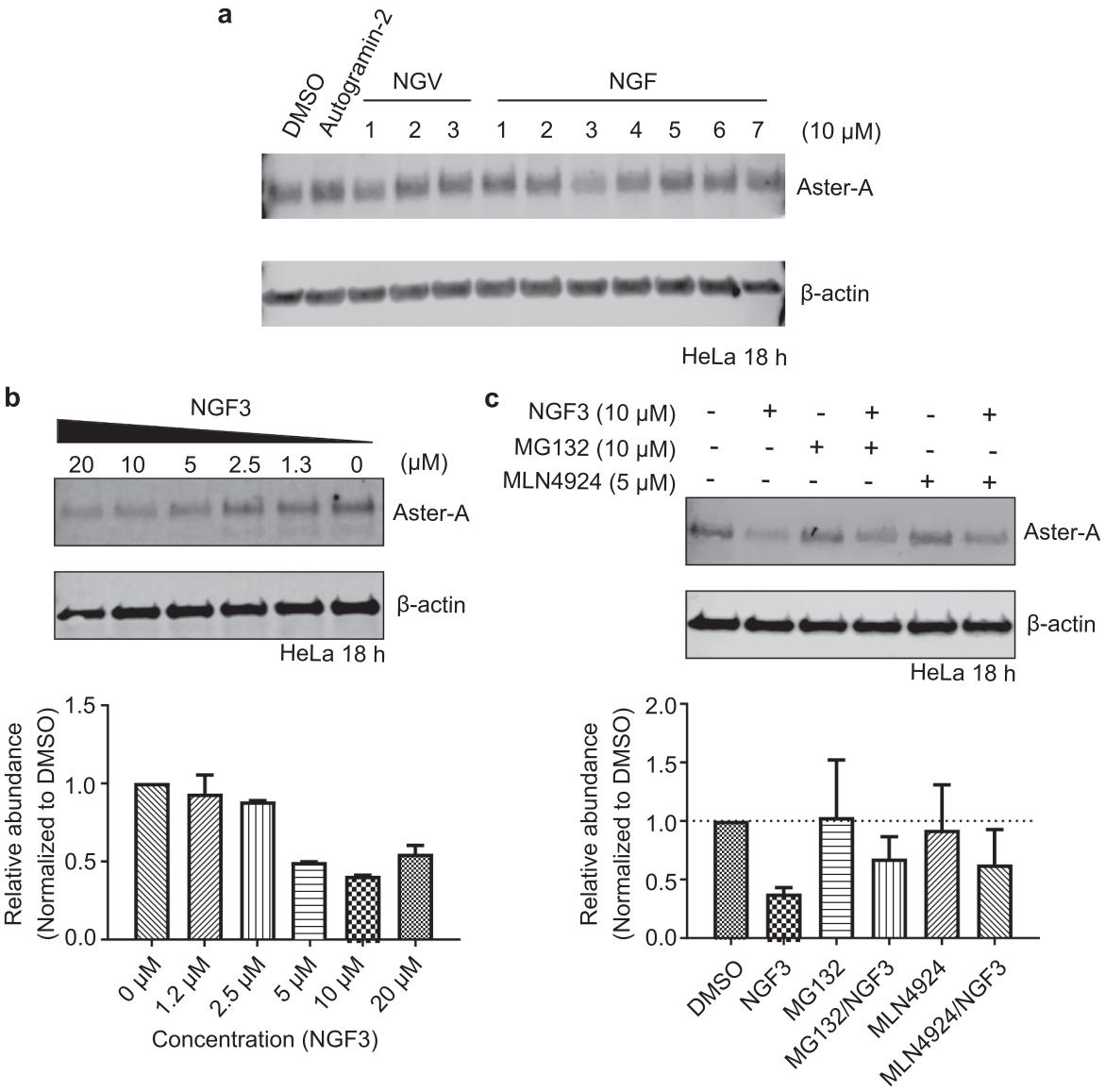

Figure 5. Effect of designed PROTACs on Aster-A protein levels. (a) Single concentration screen for Aster-A degradation in HeLa cells; (b) Dose-dependence of Aster-A degradation by **NGF-3**; (c) mechanism of Aster-A degradation by **NGF3**. All data is mean ± sem, n = 3, with representative Western blots shown.

NGF3 was explored. The degradation of Aster-A was partially blocked by MLN4924, an inhibitor of the NEDD8-activating enzyme (NAE), suggesting that an active Cullin-RING E3 ubiquitin Ligase (CRL) complex is required. Aster-A degradation induced by **NGF3** was also blocked by MG132, an established proteasome inhibitor, confirming that degradation is mediated by proteasome.

A PROTAC can exhibit various degradation efficiencies across different cell lines[22], which can be attributed to the expression levels of the target protein and E3 ligases or the mutations on the E3 ligases. Therefore, two additional cell lines, A549 human lung adenocarcinoma cells, and MCF7 human breast cancer cells constitutively expressing eGFP-LC3, were selected to investigate the effects of Aster-A degradation. The expression levels of CRBN, VHL and Aster-A vary across these three distinct cell lines (SI Figure 7a). A549 cells are predicted to display high Aster-A levels, while MCF7-eGFP-LC3 cells were selected to study the effect of Aster-A modulation on autophagy.[9,23] However, among all the tested cell lines, HeLa cells were the only cell line where the degradation of Aster-A by **NGF3** could be observed (SI Figure 7b).

To determine whether the compounds could still act as inhibitors of Aster-A in cells, we tested their ability to inhibit autophagy in MCF7-eGFP-LC3 cells.[24] Similarly to the parent compound autogramin-2. **NGF2, −3** and **−4** could all inhibit autophagy, with activity in the low μM range. **NGF2**, which contains the shortest ethylene glycol linker, displayed the most potent activity, while **NGF1** and **−5** displayed no activity, in line with their weaker and absent in vitro potency, respectively.

3. Conclusion

In conclusion, we have designed, synthesized and tested the first PROTACs for the sterol transporter Aster-A. Using the fluorescent properties of the aminophthalimide core of pomalidomide-based PROTACs, we discovered compounds that show enhanced fluorescence upon Aster-A binding. Fluorescent Aster-A probes were used in FI and FP experiments to determine K_d values, as well as to establish competition assays. In addition to biophysical experiments, the probes can also be used to qualitatively determine cellular uptake. However, a quantitative measurement is not currently possible, as the intracellular fluorescence observed is most likely a combination of cell uptake and Aster-A binding. **NGF2, −3** and **−4** still behaved as Aster-A inhibitors in cells, as assessed by their inhibition of autophagy, however only **NGF3** led to the degradation of Aster-A in a dose- and cell line-dependent manner.

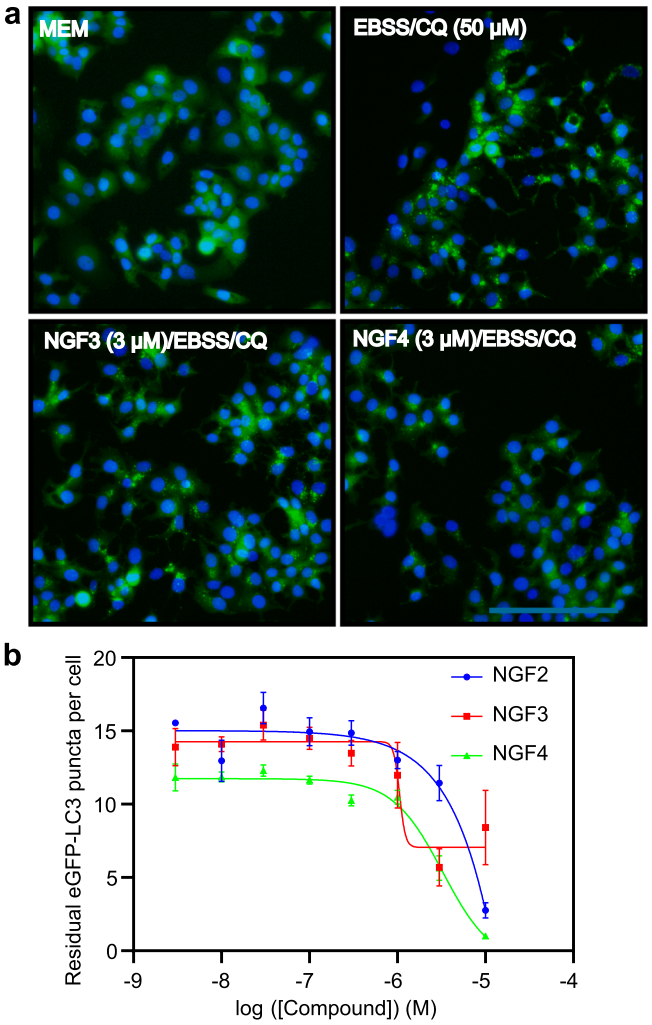

Figure 6. Aster-A ligands inhibit autophagy. All synthesized compounds were tested for inhibition of autophagy in MCF7 cells stably expressing eGFP-LC3. Autophagy was induced by amino acid starvation using EBSS. Automated microscopy and image analysis enabled quantification of puncta, representing autophagosomes; (a) representative images of active compounds and controls, scale bar = 110 μm; (b) quantification of images in (a); all data is mean ± sem (n = 3).

Further optimization of Aster-A degraders is ongoing, and will be reported in due course. A more potent degrader with broader cell line activity will be important in determining differences in phenotypic consequence between Aster-A inhibition or degradation. Overall, the different fluorescent probes reported herein will be valuable additions to study sterol transport, both in vitro and in cells. This work highlights use of aminophthalimide fluorescence for a range of applications, which warrants increased adoption by the PROTAC field.

Author contributions

N.H, L.D. and L.L. designed the project. N.H. designed and synthesized PROTACs and carried out all the cell biology experiments. L.D. expressed and purified all proteins and carried out all the biophysical experiments. S.S. performed autophagy assays. L.L. supervised the project and wrote the paper with N.H. and L.D.

CRediT authorship contribution statement

Nianzhe He: Writing – review & editing, Writing – original draft, Visualization, Methodology, Investigation, Conceptualization. **Laura Depta:** Writing – review & editing, Writing – original draft, Visualization, Methodology, Investigation, Conceptualization. **Sonja Sievers:** Methodology, Investigation. **Luca Laraia:** Writing – review & editing, Writing – original draft, Visualization, Supervision, Resources, Project administration, Funding acquisition, Conceptualization.

Declaration of competing interest

The authors declare that they have no known competing financial interests or personal relationships that could have appeared to influence the work reported in this paper.

Data availability

Data will be made available on request.

Acknowledgments

This project was funded by the Novo Nordisk Foundation (NNF19OC0055818 and NNF21OC0067188), independent research fund Denmark (9041-00241B, 9041-00248B), the Carlsberg Foundation (CF19-0072) and the European Union (ERC, ChemBioChol, 101041783). S.S. acknowledges the Max Planck Society for funding. We thank Prof. Yaowen Wu for MC7-eGFP-LC3 cells.

Appendix A. Supplementary data

Supplementary data to this article can be found online at https://doi.org/10.1016/j.bmc.2024.117673.

References

1. Depta L, Whitmarsh-Everiss T, Laraia L. Structure, function and small molecule modulation of intracellular sterol transport proteins. *Bioorg Med Chem*. 2022;68, 116856. https://doi.org/10.1016/j.bmc.2022.116856.
2. Zheng Koh DH, Saheki Y. Regulation of plasma membrane sterol homeostasis by nonvesicular lipid transport. *Contact*. 2021;4. https://doi.org/10.1177/25152564211042451, 25152564211042451.
3. Luo J, Jiang LY, Yang H, Song BL. Intracellular cholesterol transport by sterol transfer proteins at membrane contact sites. *Trends Biochem Sci*. 2019;44:273–292. https://doi.org/10.1016/j.tibs.2018.10.001.
4. Sandhu J, Li S, Fairall L, et al. Aster proteins facilitate nonvesicular plasma membrane to ER cholesterol transport in mammalian cells. *Cell*. 2018;175:514–529. e20. https://doi.org/10.1016/j.cell.2018.08.033.
5. Andersen JP, Zhang J, Sun H, et al. Aster-B coordinates with Arf1 to regulate mitochondrial cholesterol transport. *Mol Metab*. 2020;42, 101055. https://doi.org/10.1016/j.molmet.2020.101055.
6. Zhang J, Andersen JP, Sun H, et al. Aster-C coordinates with COP I vesicles to regulate lysosomal trafficking and activation of mTORC1. *EMBO Rep*. 2020;21: e49898.
7. Bandara S, Ramkumar S, Imanishi S, et al. Aster proteins mediate carotenoid transport in mammalian cells. *Proc Natl Acad Sci*. 2022;119. https://doi.org/10.1073/pnas.2200068119. e2200068119.
8. Charman M, Kennedy BE, Osborne N, Karten B. MLN64 mediates egress of cholesterol from endosomes to mitochondria in the absence of functional niemann-pick type C1 protein. *J Lipid Res*. 2010;51:1023–1034. https://doi.org/10.1194/jlr.M002345.
9. Laraia L, Friese A, Corkery DP, et al. The cholesterol transfer protein GRAMD1A regulates autophagosome biogenesis. *Nat Chem Biol*. 2019;15:710–720. https://doi.org/10.1038/s41589-019-0307-5.
10. Xiao X, Kim Y, Romartinez-Alonso B, et al. Selective Aster inhibitors distinguish vesicular and nonvesicular sterol transport mechanisms. *Proc Natl Acad Sci*. 2021; 118. https://doi.org/10.1073/pnas.2024149118. e2024149118.
11. Whitmarsh-Everiss T, Olsen AH, Laraia L. Identification of inhibitors of cholesterol transport proteins through the synthesis of a diverse, sterol-inspired compound collection. *Angew Chem Int Ed*. 2021;60:26755–26761. https://doi.org/10.1002/anie.202111639.
12. He N, Depta L, Rossetti C, et al. Selective inhibition of OSBP blocks retrograde trafficking by inducing partial golgi degradation. *bioRxiv*.. 2023 https://doi.org/10.1101/2023.04.01.534865.
13. Békés M, Langley DR, Crews CM. PROTAC targeted protein degraders: the past is prologue. *Nat Rev Drug Discov*. 2022;21:181–200. https://doi.org/10.1038/s41573-021-00371-6.
14. Banik SM, Pedram K, Wisnovsky S, Ahn G, Riley NM, Bertozzi CR. Lysosome-targeting chimaeras for degradation of extracellular proteins. *Nature*. 2020;584: 291–297. https://doi.org/10.1038/s41586-020-2545-9.
15. Takahashi D, Arimoto H. Selective autophagy as the basis of autophagy-based degraders. *Cell Chem Biol*. 2021;28:1061–1071. https://doi.org/10.1016/j.chembiol.2021.05.006.

16. Burgett AWG, Poulsen TB, Wangkanont K, et al. Natural products reveal cancer cell dependence on oxysterol-binding proteins. *Nat Chem Biol*. 2011;7:639–647. https://doi.org/10.1038/nchembio.625.
17. Steinebach C, Sosič I, Lindner S, et al. A MedChem toolbox for cereblon-directed PROTACs. *MedChemComm*. 2019;10:1037–1041. https://doi.org/10.1039/C9MD00185A.
18. Steinebach CV Sabine Anna; Vu, Lan Phuong; Bricelj, Aleša; Sosič, Izidor; Schnakenburg, Gregor; Gütschow, Michael. A Facile Synthesis of Ligands for the von Hippel–Lindau E3 Ligase. *Synthesis*. 2020;52(17):2521-2527. doi:10.1055/s-0040-1707400.
19. Hoock JGF, Rossetti C, Bilgin M, et al. Identification of non-conventional small molecule degraders and stabilizers of squalene synthase. *Chem Sci*. 2023;14:12973–12983. https://doi.org/10.1039/D3SC04064J.
20. Brownsey DK, Gafuik CJ, Kim DS, et al. Utilising the intrinsic fluorescence of pomalidomide for imaging applications. *Chem Commun*. 2023;59:14532–14535. https://doi.org/10.1039/D3CC04314B.
21. Xiao Z, Song S, Chen D, et al. Proteolysis targeting chimera (PROTAC) for macrophage migration inhibitory factor (MIF) has anti-proliferative activity in lung cancer cells. *Angew Chem Int Ed*. 2021;60:17514–17521. https://doi.org/10.1002/anie.202101864.
22. Luo X, Archibeque I, Dellamaggiore K, et al. Profiling of diverse tumor types establishes the broad utility of VHL-based ProTaCs and triages candidate ubiquitin ligases. *iScience*. 2022;25(3):103985. doi:10.1016/j.isci.2022.103985.
23. Whitmarsh-Everiss T, Laraia L. Small molecule probes for targeting autophagy. *Nat Chem Biol*. 2021;17:653–664. https://doi.org/10.1038/s41589-021-00768-9.
24. Konstantinidis G, Sievers S, Wu YW. Identification of Novel Autophagy Inhibitors via Cell-Based High-Content Screening. In: Turksen K, ed. *Autophagy in Differentiation and Tissue Maintenance: Methods and Protocols*. Springer New York; 2019:187-195. doi:10.1007/7651_2018_125.